 Bull. Chem. Soc. Jpn. Vol. 80, No. 10, 1965–1974 (2007)

Tetrameric, Tri-Titanium(IV)-Substituted Polyoxometalates with an α-Dawson Substructure as Soluble Metal Oxide Analogues. Synthesis and Molecular Structure of Three Giant "Tetrapods" Encapsulating Different Anions (Br^-, I^-, and NO_3^-)

Yoshitaka Sakai, Shoko Yoshida, Takeshi Hasegawa, Hideyuki Murakami, and Kenji Nomiya*

Department of Materials Science, Faculty of Science, Kanagawa University, Hiratsuka 259-1293

Received April 25, 2007; E-mail: nomiya@kanagawa-u.ac.jp

Preparation and structural characterization of giant "tetrapod"-shaped polyoxometalates (POMs) with approximately T_d symmetry, $[\{\alpha\text{-}P_2W_{15}Ti_3O_{59}(OH)_3\}_4\{\mu_3\text{-}Ti(H_2O)_3\}_4X]^{21-}$ (X = Br^- (**1a**), I^- (**2a**), and NO_3^- (**3a**)), consisting of four tri-titanium(IV)-substituted α-Dawson subunits, four octahedral $Ti(H_2O)_3$ bridging groups and one encapsulated anion X, are described. Sodium salts of three giant "tetrapod"-shaped POMs encapsulating different anions **1**–**3** were prepared as analytically pure crystals in 1:5 molar-ratio reactions in water of the tri-lacunary Dawson POM with the in situ-generated "TiX_4" (X = Br^-, I^-, and NO_3^-), which were prepared by the reactions of $Ti(SO_4)_2$ with BaX_2 in aqueous solution [Note: The polyoxoanion is represented by **1a**, **2a**, **3a**, ..., and the whole formula, which contains counter ions, polyoxoanion, hydrated waters, and so on, is represented by **1**, **2**, **3**, ...]. The compounds were characterized by using elemental analysis, thermogravimetric and differential thermal analyses (TG/DTA), solid-state and solution IR, solid-state and solution ^{31}P NMR spectroscopy, and X-ray crystallography. Molecular structures of **1a**–**3a** are analogous to the previously prepared POM with X = Cl^- (**4a**). The fact that encapsulation of the different anions (Cl^-, Br^-, I^-, and NO_3^-) was achieved in the central cavity of the giant "tetrapod"-shaped POM shows the cationic character of the central framework constituted by the protonated Ti–O–Ti bonds, i.e., the Ti–OH–Ti bonds. The solid-state and solution ^{31}P NMR measurements showed that **1a**–**3a** were stable in the solid-state and in DMSO, but in water, they partially decomposed. These properties of **1a**–**3a** in water are in contrast to that of **4a**.

Polyoxometalates (POMs) are molecular metal-oxide clusters, which are of current interest as soluble metal oxides and for their application to catalysis, medicine, and material sciences.[1] Site-selective substitution of the W^{VI} atoms in POMs with Ti^{IV} atoms is particularly interesting, because of the multicenter active sites formed with corner- or edge-sharing TiO_6 octahedra.[2] The ionic radius of Ti^{IV} (0.75 Å) is close to that of W^{VI} (0.74 Å), suggesting that Ti^{IV} should fit nicely into the POM framework. However, there is a significant issue of the oligomeric Ti–O–Ti anhydride formation resulting from the substitution by several Ti^{IV} atoms. The tri-Ti^{IV}-1,2,3- and the di-Ti^{IV}-1,2-substituted α-Keggin POMs, heretofore reported, have been isolated as dimeric, Ti–O–Ti-bridged anhydride forms, e.g. $[(\beta\text{-}1,2,3\text{-}SiW_9Ti_3O_{37})_2O_3]^{14-}$,[2e] $[(\alpha\text{-}1,2,3\text{-}GeW_9Ti_3O_{37})_2O_3]^{14-}$,[2f] $[(\alpha\text{-}1,2,3\text{-}PW_9Ti_3O_{37})_2O_3]^{12-}$,[2g] and $[(\alpha\text{-}1,2\text{-}PW_{10}Ti_2O_{38})_2O_2]^{10-}$,[2h] and the di-$Ti^{IV}$-1,5-substituted β-Keggin POM has been isolated as a tetrameric species, $[\{\beta\text{-}Ti_2SiW_{10}O_{39}\}_4]^{24-}$.[2j] In addtion, a few examples of Ti-substituted Dawson POMs, such as $[P_2W_{16}Ti_2O_{62}\{\mu\text{-}Ti(C_2O_4)_2\}]_2^{20-}$ [3a] and $[(TiP_2W_{15}O_{55}OH)_2]^{14-}$,[3b,c] have been reported.

From structural viewpoints, POM-based giant molecules have recently received much attention. Tungstopolyoxoanion-based giant molecules can form through self-assembly of the Keggin and Dawson lacunary units,[4] for example $[As^{III}_{12}Ce^{III}_{16}(H_2O)_{36}W_{148}O_{524}]^{76-}$,[4a] $[\{Sn(CH_3)_2(H_2O)\}_{24}\{Sn(CH_3)_2\}_{12}(A\text{-}XW_9O_{34})_{12}]^{36-}$ (X = P and As),[4b] $[(H_2P_2W_{15}O_{56})_4\{Mo_2O_2S_2(H_2O)_2\}_4\{Mo_4S_4O_4(OH)_4(H_2O)\}_2]^{28-}$,[4c] $[(UO_2)_{12}(\mu_3\text{-}O)_4(\mu_2\text{-}H_2O)_{12}(P_2W_{15}O_{56})_4]^{32-}$,[4d] $[Cu_{20}Cl(OH)_{24}(H_2O)_{12}(P_8W_{48}O_{184})]^{25-}$,[4e] and $[Nb_4O_6(\alpha\text{-}Nb_3SiW_9O_{40})_4]^{20-}$.[4f] On the other hand, a number of the molybdopolyoxoanion-based giant molecules have been also reported as mixed-valence molybdates by Müller's group,[1i,j] and their formation is based on the partial reduction of molybdate ions in aqueous media.

As to the tri-Ti^{IV}-substituted Dawson POMs, at present, there are at least four giant "tetrapod"-shaped POMs, i.e., tetrameric Ti–O–Ti-bridged anhydride forms **4a**–**7a** with or without the bridging $Ti(H_2O)_3$ octahedral groups and/or with or without an encapsulated chloride ion.[3b,5] Structure analysis of the three compounds, $[\{\alpha\text{-}1,2,3\text{-}P_2W_{15}Ti_3O_{59}(OH)_3\}_4\{\mu_3\text{-}Ti(H_2O)_3\}_4Cl]^{21-}$ (**4a**),[5a,d] $[\{\alpha\text{-}1,2,3\text{-}P_2W_{15}Ti_3O_{57.5}(OH)_3\}_4\text{-}Cl]^{25-}$ (**5a**),[5b–d] and $[\{\alpha\text{-}1,2,3\text{-}P_2W_{15}Ti_3O_{57.5}(OH)_3\}_4]^{24-}$ (**6a**)[3b] has been reported, but the presence of the species with the bridging Ti groups and without the encapsulated chloride ion **7a** has not yet been confirmed. Photo-catalytic generation of dihydrogen in the presence of glycerin under H_2SO_4-acidic conditions by **4a** and **5a** has been recently found.[5e]

In the formation of the two tetrameric, Dawson POMs with encapsulated Cl^- ion, **4a** and **5a**, one key requirement for their formation is the concentration of the titanium(IV) ion used in the reaction; POM **5a** is formed in solution with a 3:1 molar ratio of Ti^{4+}:$[B\text{-}\alpha\text{-}P_2W_{15}O_{56}]^{12-}$, while POM **4a** is formed in solution at the 10:1 molar ratio.[6]

Published on the web October 12, 2007; doi:10.1246/bcsj.80.1965

As a related compound, the monomeric tri-peroxotitanium(IV)-substituted Dawson POM Na_9[**8a**]·$16H_2O$ **8** (**8a** = [α-1,2,3-$P_2W_{15}(TiO_2)_3O_{56}(OH)_3]^{9-}$) has been prepared from a reaction with **4a** with hydrogen peroxide, but not from a reaction with **5a**.[5d] Preliminary experiments have shown that compound **8** can be used as a building block for preparation of some giant "tetrapod"-shaped POMs containing different encapsulated ions by treating the coordinated peroxo group thermally or chemically using $NaHSO_3$.

There are also significant issues involving **4a**–**6a**: the possibilities of protonation of the oxygen atoms of the Ti–O–Ti sites in intra- and/or inter-Dawson units, and the oxygen atoms of the bridging Ti octahedral sites should be taken into account. Bond valence sum (BVS) calculations of the oxygen atoms indicate that the Ti–O–Ti bonds in the intra-Dawson unit, but not the Ti–O–Ti bonds in the inter-Dawson units, are protonated in **4a**–**6a**,[5d] and the bridging Ti octahedral groups are coordinated by water molecules.[7]

This work was aimed at extending the chemistry of the tetrameric, Ti–O–Ti anhydride species of tri-titanium(IV)-susbstituted Dawson POMs **4a**–**6a**. Thus, we made an effort to find several members belonging to the giant "tetrapod"-POM family containing **7a**, and also containing different encapsulated anions (Br^-, I^-, and NO_3^-), other than the chloride ion.

Herein, we report full details of the synthesis of the novel three giant "tetrapod"-shaped POMs encapsulating different anions, [{α-$P_2W_{15}Ti_3O_{59}(OH)_3$}$_4${$\mu_3$-$Ti(H_2O)_3$}$_4$X]$^{21-}$ (X = Br^- (**1a**), I^- (**2a**), and NO_3^- (**3a**)). They were characterized by using elemental analysis, thermogravimetric and differential thermal analyses (TG/DTA), solid-state and solution IR, solid-state and solution ^{31}P NMR spectroscopy, and X-ray crystallography.

Experimental

Materials. The following reagents were used as received: $BaBr_2$, $Ba(NO_3)_2$, BaI_2·$2H_2O$, EtOH, Et_2O, CH_3CN (all from Wako), $Ti(SO_4)_2$·$4H_2O$ (Junsei), D_2O, DMSO-d_6 (Isotec). The tri-lacunary Dawson POM Na_{12}[B-α-$P_2W_{15}O_{56}$]·$19H_2O$ was prepared according to the literature and characterized.[8]

Instrumentation/Analytical Procedures. Elemental analyses were carried out by Mikroanalytisches Labor Pascher (Remagen, Germany). The samples were dried at room temperature under 10^{-3}–10^{-4} Torr overnight before elemental analysis. Infrared spectra were recorded on a Jasco 4100 FT-IR spectrometer in KBr disks at room temperature. Infrared spectra in aqueous solution were recorded on Perkin-Elmer Spectrum 100 equipped with DuraScope™ in the ATR (Attenuated Total Reflection) method at room temperature. TG/DTA were acquired using a Rigaku Thermo Plus 2 series TG/DTA TG8120 instrument. TG/DTA measurements were run under air with a temperature ramp of 4 °C per min between 30 and 500 °C.

^{31}P{^{1}H} NMR (161.70 MHz) spectra in solution were recorded in 5 mm outer diameter tubes on a JEOL JNM-EX 400 FT-NMR spectrometer with a JEOL EX-400 NMR data processing system. ^{31}P{^{1}H} NMR spectra were measured in D_2O or DMSO-d_6 solution with reference to an external standard of 25% H_3PO_4 in H_2O in a sealed capillary. ^{31}P NMR signals were shifted by −0.101 ppm by using 85% H_3PO_4 as a reference instead of 25% H_3PO_4. ^{31}P CPMAS NMR (121.00 MHz) spectra were recorded in 6 mm outer diameter tubes on a JEOL JNM-ECP 300 FT-NMR spectrometer with JEOL ECP-300 NMR data processing system. These spectra were referenced to an external standard, $(NH_4)_2HPO_4$. Chemical shifts are reported as negative for resonances upfield of $(NH_4)_2HPO_4$ (δ 1.60).

Preparations. **$Na_{21-x}H_x$[1a]·yH_2O (x = 0–4, y = 68–69) (1):** To a solution of $Ti(SO_4)_2$·$4H_2O$ (2.0 g, 6.41 mmol) dissolved in water (50 mL) by warming was added $BaBr_2$ (3.2 g, 10.8 mmol). The white powder ($BaSO_4$) that formed while stirring for 1 h in an ice bath was filtered off through a membrane filter (JG 0.2 μm). To the clear colorless filtrate was added solid Na_{12}[B-α-$P_2W_{15}O_{56}$]·$19H_2O$ (5.0 g, 1.15 mmol). The clear pale yellow solution was stirred for 1 h on a water bath at about 80 °C. After cooling to room temperature, the solution was concentrated to a volume of about 10 mL with a rotary evaporator at 40 °C. The volume was further concentrated to ca. 6 mL on a water bath at 90 °C. The resulting clear yellow solution was left to stand at room temperature for two days. A pale yellow crystalline solid that formed was collected on a glass filter (G3) and dried in vacuo for 2 h. At this stage, crude **1**, which was a pale yellow powder, was obtained in ca. 2.9 g yield. All of the pale yellow powder was dissolved in water (5 mL) on a water bath at 80 °C, and then the solution was stirred for 10 min at 80 °C. After cooling to room temperature, the pale yellow solution was added to 150 mL of EtOH. A white powder that formed while stirring for 15 min was collected on a membrane filter (JG 0.2 μm) and washed with Et_2O (50 mL × 3) (as 1st crop in 0.9 g yield). To the filtrate was added 350 mL of Et_2O, and the resulting white suspension was stirred for 15 min. The white precipitate was collected on a membrane filter (JG 0.2 μm) and washed with Et_2O (50 mL × 3) (as 2nd crop in 1.4 g yield). A white powder of the crude product was obtained in combined 2.3 g yield.

Crystallization; The crude product (4.0 g) was dissolved in 3 mL of water on a water bath at 90 °C. The clear pale yellow solution was slowly concentrated at room temperature. After about five days, clear colorless granular crystals formed, and they were used for X-ray diffraction measurement. The crystalline samples were collected on a membrane filter (JG 0.2 μm) and washed quickly with ice-cooled water (1 mL × 2), ice-cooled EtOH (5 mL × 2) and then Et_2O (30 mL × 3). During this washing process, the crystalline samples became white powder. The resulting white powder was further washed with a mixed solvent of H_2O/EtOH = 1/9 (10 mL × 1) and then Et_2O (50 mL × 3), and dried in vacuo for 2 h. Compound **1**, obtained in 12.8% yield (1.15 g scale), is highly soluble in water, soluble in DMSO, sparingly soluble in EtOH, insoluble in Et_2O, and used for the following characterization.

Microanalysis; Calculated values were fitted within allowed errors for all x = 0–4 in $Na_{21-x}H_x$[{$P_2W_{15}Ti_3O_{59}(OH)_3$}$_4${$\mu_3$-$Ti(H_2O)_3$}$_4$Br]·$4H_2O$. Calcd for x = 0 or $H_{44}O_{264}Na_{21}P_8Ti_{16}W_{60}Br_1$: H, 0.26; O, 25.03; Na, 2.86; P, 1.47; Ti, 4.54; W, 65.37; Br, 0.47%; calcd for x = 4 or $H_{48}O_{264}Na_{17}P_8Ti_{16}W_{60}Br_1$: H, 0.29; O, 25.16; Na, 2.33; P, 1.48; Ti, 4.56; W, 65.71; Br, 0.48%. Found: H, 0.44; O, 25.2; Na, 2.72; P, 1.38; Ti, 4.60; W, 64.8; Br, 0.3%; total 99.44%. A weight loss of 6.46% was observed during the course of drying at room temperature at 10^{-3}–10^{-4} Torr overnight before analysis, suggesting the presence of ca. 65 weakly solvated or adsorbed water molecules. TG/DTA data under atmospheric conditions: a weight loss of 7.79% below 150.4 °C was observed with endothermic peaks at 63.7 and 75.8 °C; calcd 7.81% for y = 78 in $Na_{17}H_4$[**1a**]·yH_2O. IR (KBr disk, polyoxometalate region): 1090(vs), 952(vs), 913(s), 822(vs), 743(s), 649(vs,br), 561(m), 529(w) cm^{-1}. IR in aqueous solution

(4000–550 cm^{-1} region): 3501(m), 2983(m), 1623(m), 1090(vs), 954(vs), 906(s), 822(vs), 611(vs), 597(vs), 561(vs) cm^{-1}. ^{31}P CPMAS NMR: δ −6.72, −13.70. ^{31}P NMR (DMSO-d_6, 19.5 °C): δ −6.82, −13.61. ^{31}P NMR (D_2O, 20.6 °C): δ −6.93, −13.79 (main peaks), −7.03, −7.27 (minor peaks).

$Na_{21-x}H_x$[2a]·yH_2O (x = 0–4, y = 89–90) (2): To a solution of $Ti(SO_4)_2 \cdot 4H_2O$ (2.0 g, 6.41 mmol) dissolved in water (50 mL) by warming was added $BaI_2 \cdot 2H_2O$ (4.8 g, 11.2 mmol). The white powder ($BaSO_4$) that formed while stirring for 1 h in an ice bath was filtered off through a membrane filter (JG 0.2 μm). To the clear yellow filtrate was added solid Na_{12}[B-α-$P_2W_{15}O_{56}$]·$19H_2O$ (5.0 g, 1.15 mmol). The clear yellow solution was stirred for 1 h on a water bath at 80 °C. After cooling to room temperature, the solvent was evaporated by using a rotary evaporator at 40 °C, until a powder began to form (to ca. 10 mL volume). The resulting suspension was warmed on a water bath at 90 °C until the powder redissolved. The clear brown solution was left to stand at room temperature overnight. The yellow crystalline solid that formed was collected on a glass filter (G3.5). All of the yellow crystalline solid was dissolved in 3 mL of water. The clear yellow solution was added to 150 mL of CH_3CN. After stirring for 10 min, 350 mL of Et_2O was added to the solution. The pale yellow powder that precipitated during stirring for 30 min was collected on a membrane filter (JG 0.2 μm), washed with Et_2O (50 mL × 3) and dried in vacuo for 2 h. At this stage, the crude **2** was obtained as a pale yellow powder in ca. 2.9 g yield.

Crystallization; The crude product (5.0 g) was dissolved in 3 mL of a water on a water bath at 90 °C. The pale yellow solution was passed through a folded filter paper (Whatman No. 4), and then the filtrate was slowly concentrated at room temperature. After about six days, clear pale yellow granular crystals formed, and they were used for X-ray diffraction measurement. The crystalline sample was collected on a membrane filter (JG 0.2 μm) and washed quickly with ice-cooled water (1 mL × 2), ice-cooled CH_3CN (5 mL × 1) and then Et_2O (50 mL × 3). After this washing process, the resulting pale yellow powder was further washed with a mixed solvent of H_2O/CH_3CN = 1/9 (10 mL × 1) and then Et_2O (50 mL × 3), and dried in vacuo for 2 h. Compound **2**, obtained in 9.37% yield (0.85 g scale), is highly soluble in water, soluble in DMSO, sparingly soluble in CH_3CN and EtOH, insoluble in Et_2O.

Microanalysis; Calculated values were fitted within allowed errors for all x = 0–4 in $Na_{21-x}H_x$[{$P_2W_{15}Ti_3O_{59}(OH)_3$}$_4${$\mu_3$-$Ti(H_2O)_3$}$_4$]·$12H_2O$. Calcd for x = 0 or $H_{60}O_{272}Na_{21}P_8Ti_{16}W_{60}I_1$: H, 0.35; O, 25.50; Na, 2.83; P, 1.45; Ti, 4.49; W, 64.63; I, 0.74%; calcd for x = 4 or $H_{64}O_{272}Na_{17}P_8Ti_{16}W_{60}I_1$: H, 0.38; O, 25.63; Na, 2.30; P, 1.46; Ti, 4.51; W, 64.97; I, 0.75%. Found: H, 0.47; O, 25.5; Na, 2.63; P, 1.40; Ti, 4.64; W, 64.8; I, 0.42%; total 99.86%. A weight loss of 7.58% was observed during the course of drying at room temperature at 10^{-3}–10^{-4} Torr overnight before analysis, suggesting the presence of ca. 78 weakly solvated or adsorbed water molecules. TG/DTA data under atmospheric conditions: a weight loss of 8.20% below 151.0 °C was observed with an endothermic peak at 63.2 °C; calcd 8.19% for y = 83 in $Na_{17}H_4$[**2a**]·yH_2O. IR (KBr disk, polyoxometalate region): 1090(vs), 953(vs), 913(s), 822(vs), 743(s), 649(vs,br), 561(m), 528(m) cm^{-1}. ^{31}P CPMAS NMR: δ −6.72, −13.57. ^{31}P NMR (DMSO-d_6, 19.1 °C): δ −6.74, −13.50. ^{31}P NMR (D_2O, 20.3 °C): δ −6.81, −13.82 (main peaks), −7.33 ppm (minor peak).

$Na_{21-x}H_x$[3a]·yH_2O (x = 2–6, y = 79–83) (3): To a solution of $Ti(SO_4)_2 \cdot 4H_2O$ (1.8 g, 5.77 mmol) dissolved in water (50 mL) by warming was added $Ba(NO_3)_2$ (2.8 g, 10.7 mmol). After stirring for 1 h in an ice bath, $BaSO_4$ was filtered off through a Buchner funnel (Whatman No. 2). Solid Na_{12}[B-α-$P_2W_{15}O_{56}$]·$19H_2O$ (5.0 g, 1.15 mmol) was added to the clear colorless filtrate, followed by stirring for 1 h on a water bath at 80 °C. The resulting suspension was cooled to room temperature, and the white powder that formed was filtered off through a membrane filter (JG 0.2 μm). The clear colorless filtrate was concentrated to a volume of 5 mL with a rotary evaporator at 40 °C. The volume was further reduced to 3 mL on a water bath at 90 °C. The clear pale yellow solution was left to stand at room temperature for two days. The colorless crystalline solid was collected on a glass filter (G3) and dried in vacuo for 2 h. At this stage, crude **3** as a white powder was obtained in ca. 1.8 g yield.

Crystallization; The crude product (4.0 g) was dissolved in 2 mL of water on a water bath at 90 °C. The colorless solution was slowly concentrated at room temperature. After about nine days, clear colorless granular crystals formed and used for X-ray diffraction measurement. The crystalline samples collected on a membrane filter (JG 0.2 μm) were washed quickly with ice-cooled water (1 mL × 2), ice-cooled EtOH (5 mL × 2) and then Et_2O (50 mL × 3), and dried in vacuo for 2 h. During the washing process, the crystals became a white powder. Compound **3**, obtained in ca. 14% yield (1.6 g scale), is highly soluble in water, soluble in DMSO, sparingly soluble in EtOH, insoluble in Et_2O and used for the following characterization.

Microanalysis; Calculated values were fitted within allowed errors for all x = 2–6, z = 2–6 in $Na_{21-x}H_x$[{$P_2W_{15}Ti_3O_{59}(OH)_3$}$_4${$\mu_3$-$Ti(H_2O)_3$}$_4(NO_3)$]·$zH_2O$. Calcd for x = 2, z = 2 or $H_{42}N_1O_{265}Na_{19}P_8Ti_{16}W_{60}$: H, 0.25; N, 0.08; O, 25.27; Na, 2.60; P, 1.48; Ti, 4.57; W, 65.75%; calcd for x = 6, z = 6 or $H_{54}N_1O_{269}Na_{15}P_8Ti_{16}W_{60}$: H, 0.32; N, 0.08; O, 25.68; Na, 2.06; P, 1.48; Ti, 4.57; W, 65.81%. Found: H, 0.37; N, 0.08; O, 25.30; Na, 2.30; P, 1.37; Ti, 4.59; W, 65.4%; total 99.41%. A weight loss of 7.66% was observed during the course of drying at room temperature at 10^{-3}–10^{-4} Torr overnight before analysis, suggesting the presence of ca. 78 weakly solvated or adsorbed water molecules. TG/DTA data under atmospheric conditions: a weight loss of 8.36% below 151.1 °C was observed with endothermic peaks at 63.7, 91.4, and 107.4 °C; calcd 8.36% for y = 86 in Na_{21}[{$P_2W_{15}Ti_3O_{59}(OH)_3$}$_4${$\mu_3$-$Ti(H_2O)_3$}$_4(NO_3)$]·$yH_2O$. IR (KBr disk, polyoxometalate region): 1384(s), 1090(vs), 953(vs), 910(s), 824(vs), 653(vs), 560(m), 531(m) cm^{-1}. IR in aqueous solution (4000–550 cm^{-1} region): 3504(m), 1624(m), 1350(m), 1090(s), 955(s), 911(s), 825(s), 599(vs), 580(vs), 556(vs) cm^{-1}. ^{31}P CPMAS NMR: δ −6.60, −13.45. ^{31}P NMR (DMSO-d_6, 20.1 °C): δ −7.06, −13.33. ^{31}P NMR (D_2O, 20.5 °C): δ −6.96, −13.90 (main peaks), −7.12, −7.46 (minor peaks).

$Na_{21-x}H_x$[4a]·yH_2O (x = 1–4, y = 63–66) (4): Synthesis and characterization are reported elsewhere.[5a] IR in aqueous solution (4000–550 cm^{-1} region): 3493(m), 3059(m), 1623(m), 1090(s), 954(s), 906(s), 821(s), 615(s), 598(s) cm^{-1}.

X-ray Crystallography. A clear colorless granular crystal of **1**, a clear pale yellow granular crystal **2** and a clear colorless granular crystal of **3** were surrounded by liquid paraffin (Paratone-N) to prevent their degradation. Data was collected on a Bruker SMART APEX CCD diffractometer. Intensity data were automatically corrected for Lorentz and polarization effects during integration. The structures were solved by direct methods (program SHELXS-97)[9a] followed by subsequent difference Fourier calculations and refined by full-matrix, least-square procedure (program SHELXL-97).[9b] Absorption correction was performed with

Table 1. Crystal Data for Compounds **1**–**3**

Parameter	$Na_{17}H_4$[**1a**]·$79H_2O$ (**1**)	$Na_{17}H_4$[**2a**]·$80H_2O$ (**2**)	$Na_{17}H_4$[**3a**]·$78H_2O$ (**3**)
Empirical formula	$H_{198}Br_1Na_{17}O_{339}P_8Ti_{16}W_{60}$	$H_{200}I_1Na_{17}O_{340}P_8Ti_{16}W_{60}$	$H_{196}N_1Na_{17}O_{341}P_8Ti_{16}W_{60}$
fw	18139.48	18204.49	18103.57
Temp/K	90(2)	90(2)	90(2)
Wavelength/Å	0.71073	0.71073	0.71073
Crystal system	Monoclinic	Monoclinic	Monoclinic
Space group	$P2_1/c$	$P2_1/c$	$P2_1/c$
Unit cell dimensions (Å, deg)	$a = 26.706(2)$	$a = 26.734(2)$	$a = 26.697(2)$
	$b = 50.362(4)$	$b = 50.319(4)$	$b = 50.280(4)$
	$c = 27.627(2)$	$c = 27.579(2)$	$c = 27.718(2)$
	$\beta = 94.4870(10)$	$\beta = 94.506(2)$	$\beta = 94.388(2)$
Volume/Å^3	37044(5)	36986(5)	37098(6)
Z	4	4	4
D_{calcd}/Mg m^{-3}	3.252	3.269	3.241
Abs coeff (mm^{-1})	19.136	19.141	19.001
$F(000)$	32176	32288	32120
Crystal size/mm^3	0.41 × 0.25 × 0.11	0.24 × 0.13 × 0.11	0.20 × 0.18 × 0.15
θ range for data collcn/deg	0.76 to 28.35°	0.76 to 28.37°	0.76 to 28.39°
Index ranges	$-35 \le h \le 35$, $-67 \le k \le 67$, $-36 \le l \le 36$	$-35 \le h \le 35$, $-67 \le k \le 67$, $-36 \le l \le 36$	$-35 \le h \le 35$, $-67 \le k \le 67$, $-37 \le l \le 35$
Reflcns collcd	399429	495816	441962
Indepndt reflcns	91908 [R(int) = 0.0866]	92256 [R(int) = 0.1173]	92433 [R(int) = 0.1042]
Refinement method	full-matrix least-squares on F^2	full-matrix least-squares on F^2	full-matrix least-squares on F^2
Data/restraints/parameters	91908/2646/3970	92256/2652/3979	92433/2658/3988
Goodness-of-fit on F^2	1.023	1.029	1.112
Final R indices [$I > 2\sigma(I)$]	$R1 = 0.0622$, $wR2 = 0.1578$	$R1 = 0.0629$, $wR2 = 0.1577$	$R1 = 0.0905$, $wR2 = 0.2227$
R indices (all data)	$R1 = 0.0948$, $wR2 = 0.1790$	$R1 = 0.1050$, $wR2 = 0.1837$	$R1 = 0.1298$, $wR2 = 0.2483$
Largest diff. peak and hole/e Å^{-3}	14.053 and −6.664	9.934 and −7.398	19.406 and −10.886

SADABS (empirical absorption correction).[9c] Crystal data of **1**–**3** are listed in Table 1.

The final cycle of refinement, including the atomic coordinates and anisotropic thermal parameters, converged at $R = 0.0622$ and $R_w = 0.1578$ for **1**, $R = 0.0629$ and $R_w = 0.1577$ for **2**, and $R = 0.0905$ and $R_w = 0.2227$ for **3**, all for $I > 2\sigma(I)$. No hydrogens were included in the refinement. We obtained the best crystallographic refinement results (lowest residual electron density) by assigning 17 sodium counter ions (full occupancy for Na1–Na17), for **1**–**3**. The 60 tungsten atoms, the 16 titanium atoms, the 8 phosphorus atoms and the one X atom or group (Br, I, and NO_3) were clearly identified for **1**–**3**. Thus, the main features of the molecular structures of POMs were clear. However, it is very frequently impossible in POM chemistry due to disorder to locate and assign all counteractions and water molecules of crystallization unequivocally by single-crystal X-ray diffraction.

Further details on the crystal structure investigation may be obtained from the Fachinformationszentrum Karlsruhe, 76344 Eggenstein-Leopoldshafen, Germany (fax: (+49)7247-808-666); e-mail crysdata@fiz-karlsruhe.de, on quoting the depository numbers. CSD-417624 (formula/code: yos225s), CSD-417623 (yos224s), and CSD-417622 (yos223s) for complexes **1**–**3**, respectively.

Results and Discussion

Synthesis and Compositional Characterization. Sodium salts of three giant "tetrapod"-shaped titanium(IV)-substituted Dawson POMs encapsulating the different anions X, $Na_{21-x}H_x$[**A**]·yH_2O (**A** = $[\{P_2W_{15}Ti_3O_{59}(OH)_3\}_4\{\mu_3\text{-}Ti(H_2O)_3\}_4X]^{21-}$) X = Br^- (**1**), I^- (**2**), NO_3^- (**3**), were prepared by 1:5 molar ratio reactions in water of tri-lacunary Dawson POM with the in-situ "TiX_4" (X = Br^-, I^-, and NO_3^-), which was prepared by treating $Ti(SO_4)_2$ with BaX_2 in aqueous solutions. They were obtained both as bulk powder samples and crystalline samples. Characterization data of the bulk powder samples were identical with those of the crystalline samples. Colorless granular crystals of **1** and **3** and pale yellow granular crystals of **2** were obtained in 9–15% yields.

The formation of these POMs is represented in Eq. 1.

$$16\ \text{"}Ti^{4+}\text{"} + X^- + 4[\text{B-}\alpha\text{-}P_2W_{15}O_{56}]^{12-} + 36H_2O \rightarrow [\{P_2W_{15}Ti_3O_{59}(OH)_3\}_4\{\mu_3\text{-}Ti(H_2O)_3\}_4X]^{21-} + 36H^+. \quad (1)$$

These complexes were characterized by using elemental analyses, TG/DTA, solid-state and solution IR, solid-state and solution ^{31}P NMR spectroscopy and single-crystal X-ray diffraction analysis. The samples for elemental analyses were dried at room temperature under vacuum of 10^{-3}–10^{-4} Torr overnight. All elements were observed, including oxygen, to the total analyses of 99.44, 99.86, and 99.41% for **1**–**3**, respectively. Here, it should be noted that, in **3**, a trace analysis for N was separately performed under the required detection limits of 0.01%, and a satisfactory result was obtained (see Experimental). Also, it should be noted that more than one formula containing counter ions and crystallization waters for **1**–**3** can be determined, because the compound has a very large molecular weight; however, full elemental analysis including O analysis was carried out. From the analytical data of the dried samples under 10^{-3}–10^{-4} Torr overnight, the compositions were estimated to be $Na_{21-x}H_x$[**1a**]·$4H_2O$ ($x = 0$–4)

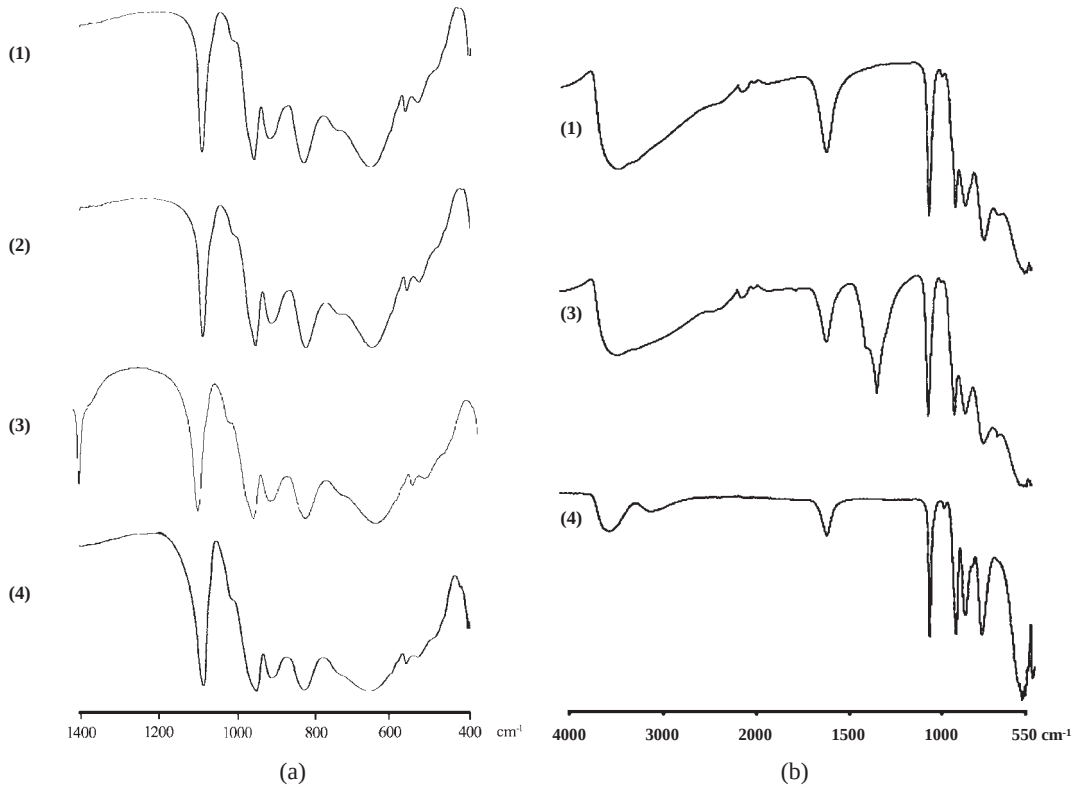

Fig. 1. (a) IR spectra in the POM region of (1400–400 cm^{-1}), measured as KBr disks, of **1**, **2**, **3**, and **4**. (b) IR spectra in the 4000–550 cm^{-1} region, measured by the ATR method, of **1**, **3**, and **4**.

for **1**, $Na_{21-x}H_x$[**2a**]·$12H_2O$ ($x = 0$–4) for **2**, and $Na_{21-x}H_x$[**3a**]·zH_2O ($x = 2$–6, $z = 2$–6) for **3**. The weight losses observed during drying before analysis were 6.46% for **1**, which corresponds to ca. 65 weakly solvated and/or adsorbed water molecules, 7.58% for **2**, which corresponds to ca. 78 water molecules, and 7.66% for **3**, which corresponds to ca. 78 water molecules. On the other hand, in the TG/DTA measurements performed under atmospheric conditions, a weight loss of 7.79% observed below 150 °C for **1** corresponded to 78 water molecules, that of 8.20% observed below 151 °C for **2** corresponded to 83 water molecules and that of 8.36% observed below 151 °C for **3** corresponded to 86 water molecules. Thus, the numbers of water molecules observed by TG/DTA measurements under atmospheric conditions are almost consistent with the sum of the water molecules found in the elemental analyses plus the water molecules corresponding to the weight losses observed during the course of drying before analyses (see Experimental).

Solid-state IR measurements (Fig. 1) of **1**–**3** show the spectral patterns characteristic of the Dawson POM framework.[10] The IR spectra of **1**–**3** in the Dawson POM region are very similar to that of the related POM encapsulating Cl^- ion, $Na_{21-x}H_x$[**4a**]·yH_2O ($x = 1$–4, $y = 63$–66) (**4**),[5a] especially with regards to the P–O bands (1090 cm^{-1} for **1**–**4**), the bands assignable to M–$O_{terminal}$ oxygen atoms (952 cm^{-1} for **1**, 953 cm^{-1} for **2**, 954 cm^{-1} for **3** and 954 cm^{-1} for **4**), the bands assignable to corner-sharing M–O–M oxygen atoms (913 cm^{-1} for **1**, 913 cm^{-1} for **2**, 911 cm^{-1} for **3** and 914 cm^{-1} for **4**) and the bands assignable to edge-sharing M–O–M oxygen atoms (822 cm^{-1} for **1**, 822 cm^{-1} for **2**, 820 cm^{-1} for **3** and 828 cm^{-1} for **4**). Furthermore, the Ti–O–Ti vibration bands of inter-Dawson units observed in **1**–**3** were also similar to that of **4** (649 cm^{-1} for **1**, 649 cm^{-1} for **2**, 644 cm^{-1} for **3**, and 656 cm^{-1} for **4**). Finally, the IR spectrum of **3** showed a band due to the encapsulated NO_3^- anion at 1384 cm^{-1}.

Molecular Structures. The crystal system (monoclinic), the space group ($P2_1/c$) and a disorder-free POM unit provided a straightforward solution of the structure as well as refinement. The crystals of **1**–**3** contain discrete polyoxoanions, sodium cations and lattice water molecules, all on general positions in this space group. The 17 sodium cations for **1**–**3**, respectively, could be identified in the crystal structures (see Experimental).

Structure analysis showed that the molecular structures had four Dawson units through Ti–O–Ti bonds and the four bridging Ti octahedral groups arranged in T_d symmetry, as displayed in Fig. 2 for **1a**–**3a**, respectively. The molecular structures of **1a**–**3a** are composed of one encapsulated X anion ($X = Br^-$, I^-, and NO_3^-) and four "$P_2W_{15}Ti_3O_{62}$" Dawson units (designated as A, B, C, and D) linked to four bridging Ti octahedral groups (designated as W, X, Y, and Z), each Dawson unit of which has the same α-Dawson structure [α-1,2,3-$P_2W_{15}Ti_3O_{62}$]$^{12-}$. These features are essentially the same as that of the recently reported, giant "tetrapod"-shaped POM with $X = Cl^-$ (**4a**).[5a] Three TiO_6 octahedra (Ti_3 cap) in each "$P_2W_{15}Ti_3$" Dawson unit replace three edge-sharing WO_6 octahedra (W_3 cap) of [α-$P_2W_{18}O_{62}$]$^{6-}$. The partial structure containing one Dawson unit, to which the three Ti octahedral groups are linked is depicted in Fig. 3 for **1a**, as an example. The three terminal oxygen atoms of the Ti_3 cap

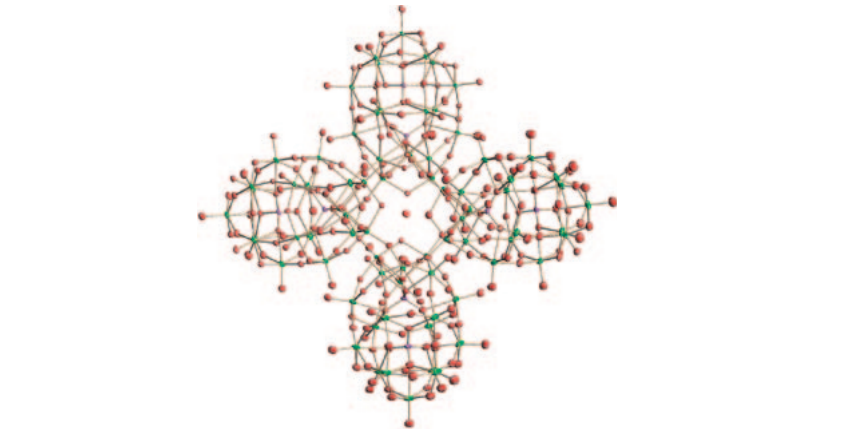

(1a)

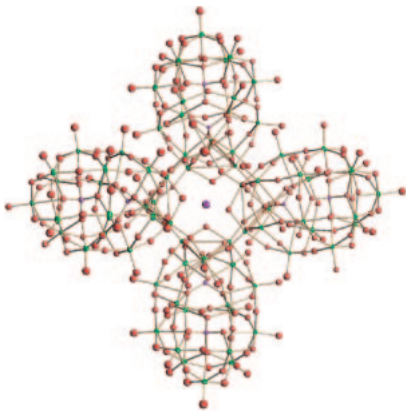

(2a)

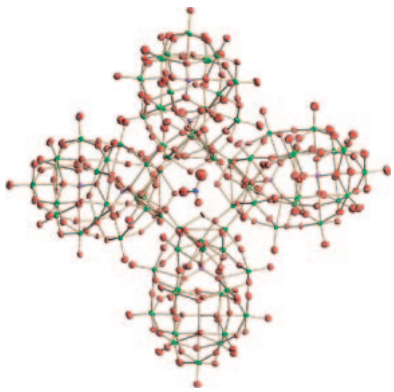

(3a)

Fig. 2. Molecular structures with 50% probability ellipsoids of **1a**, **2a**, and **3a** containing an Br^- ion, I^- ion, and NO_3^- ion in the central cavity, respectively.

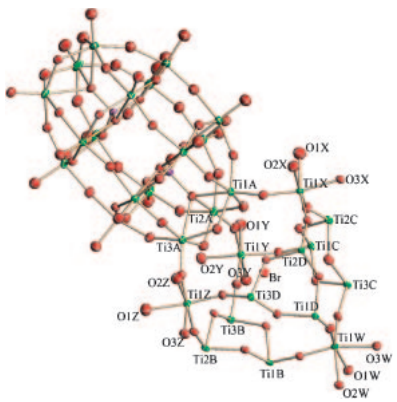

Fig. 3. Partial structure of **1a** showing one Dawson-POM unit A, to which the three Ti octahedral groups (X, Y, and Z) are linked. The Dawson unit A is linked with other Dawson units (B, C, and D) through Ti–O–Ti bonds with the bridging Ti octahedral groups.

are linked to three different Ti octahedral groups through Ti–O–Ti bonds. In other words, Dawson unit A is connected to the Ti octahedral groups (X, Y, and Z), Dawson unit B is connected to the Ti octahedral groups (Y, Z, and W), Dawson unit C is connected to the Ti octahedral groups (Y, X, and W), and Dawson unit D is connected to the Ti octahedral groups (W, X, and Z).[5a]

The four bridging Ti octahedral groups occupy the corner of a large tetrahedron, and one anion is encapsulated inside. Thus, the giant "tetrapod" molecule with approximately T_d symmetry is constructed. The three Ti atoms and fifteen W atoms for each Dawson unit, and the bridging Ti octahedral groups all have conventional octahedral coordination. The polyhedral representation for the present polyoxoanion is shown in Fig. 4.

Selected bond distances (Å) and angles (°) around the titanium(IV) centers for the Dawson-POM unit A in **1a**–**3a** (Tables S1–S3), and average bond distances (Å) and angles (°) [range] for the Dawson-POM unit A in **1a**–**3a** (Tables S4–S6) are given in Supporting Information. Selected bond distances (Å) and angles (°) around the titanium(IV) centers for the Dawson-POM unit A in **1a**–**3a** are in approximately the same range and are comparable to those in **4a**.[5a] In the W_3 cap of Dawson-POM unit A in **1a**–**3a**, the W–Ot (Ot: terminal oxygen), W–Oe (Oe: edge-sharing oxygen), W–Oc (W belt) (Oc: corner-sharing oxygen) and W–Oa (Oa: oxygen coordinated to P atom) distances are in the normal range.[1b] Dawson unit A contained two central P atoms in an almost regular tetrahedral environment of PO_4.

The Br^- and I^- ions in **1a** and **2a**, respectively, are en-

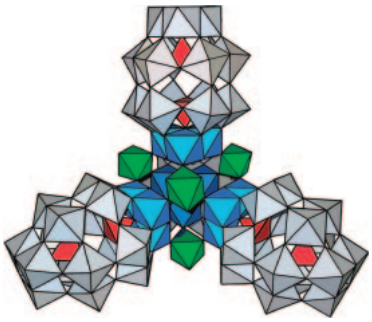

Fig. 4. Polyhedral representation of the giant "terapod" polyoxoanion with approximately T_d symmetry, which composed of the WO_6 octahedra (gray), the internal PO_4 tetrahedra (red), the TiO_6 octahedra in the Ti_3 cap (blue), and the bridging TiO_6 octahedra (green). The encapsulated anion in the central tetrahedral cavity is hidden.

capsulated in the central tetrahedral site, just like the Cl^- ion encapsulated in **4a**. Here, it should be noted that the N–O bond distances of the encapsulated NO_3^- ion in **3a** (N1–O1N 1.20(3), N1–O2N 1.29(4), N1–O3N 1.25(3) Å) and the O–N–O angles (O2N–N1–O1N 120(3), O3N–N1–O2N 113(2), O1N–N1–O3N 123(2)°, total 356°) are comparable to those of the crystal of $HNO_3 \cdot H_2O$ (N–O bond distances (N–O1 1.22, N–O2 1.22, N–O3 1.29 Å) and O–N–O angles (O2–N–O1 127, O3(···H)–N–O2 116.5, O1–N–O3(···H) 116.5°, total 360°)).[11]

The bond valence sums (BVS: see Tables S7–S9),[12] calculated based on the observed bond distances for Dawson units A, B, C, and D in **1a**–**3a**, were reasonably consistent with the formal valences of Ti^{4+}, W^{6+}, and P^{5+}, similar to **4a**. The BVS for the Ti atoms of the four bridging Ti octahedral groups were in the range of 4.082–4.378, which corresponds to the formal valence +4. The BVS for the N atom of the encapsulated NO_3^- ion (4.975) corresponded to the formal valence +5.

The protonation of all Ti–O–Ti bridges of the Ti_3 cap within the Dawson units for **4a**–**6a**, but not the Ti–O–Ti bridges between the Dawson units, has been confirmed using BVS calculations.[3b,5d] This is also the case for the surface edge-sharing oxygen atoms of the Ti_3 cap within the Dawson units in **1a**–**3a** (see Tables S7–S9). The fact that encapsulation of the different anions (Cl^-, Br^-, I^-, and NO_3^-) has been realized in the central cavity of the giant "tetrapod"-shaped POM elucidates the cationic character of the central framework constituted by the protonated Ti–O–Ti bonds, i.e., the Ti–OH–Ti bonds.

The formula of the giant "tetrapod"-POM with the bridging Ti octahedral groups also depends if the oxygen atoms attached to the bridging Ti octahedral group are due to OH^- or H_2O. BVS calculations of such oxygen atoms (e.g., O1X, 0.481; O2X, 0.427; O3X, 0.476 in **3a** (see Tables S7–S9)) suggest that these oxygen atoms are reasonably assignable to water molecules (≈1 expected for the OH^- group).[7b,c] Thus, the present molecular formulas of **1a**–**3a** are represented as $[\{\alpha\text{-}1,2,3\text{-}P_2W_{15}Ti_3O_{59}(OH)_3\}_4\{\mu_3\text{-}Ti(H_2O)_3\}_4X]^{21-}$ (X = Br^-, I^-, NO_3^-, Cl^-). As for the interpretation of BVS values of the oxygen atoms coordinated to the bridging Ti atoms, i.e., due to OH^- or H_2O, they have been erroneously assigned to the OH^- groups in the previous formula of **4a**.[5a,d] Thus, the apparent charge for the same polyoxoanion **4a** in the solid state is due to protonation of the Ti–O–Ti site within the Dawson subunit and the bridging Ti octahedral site.[5]

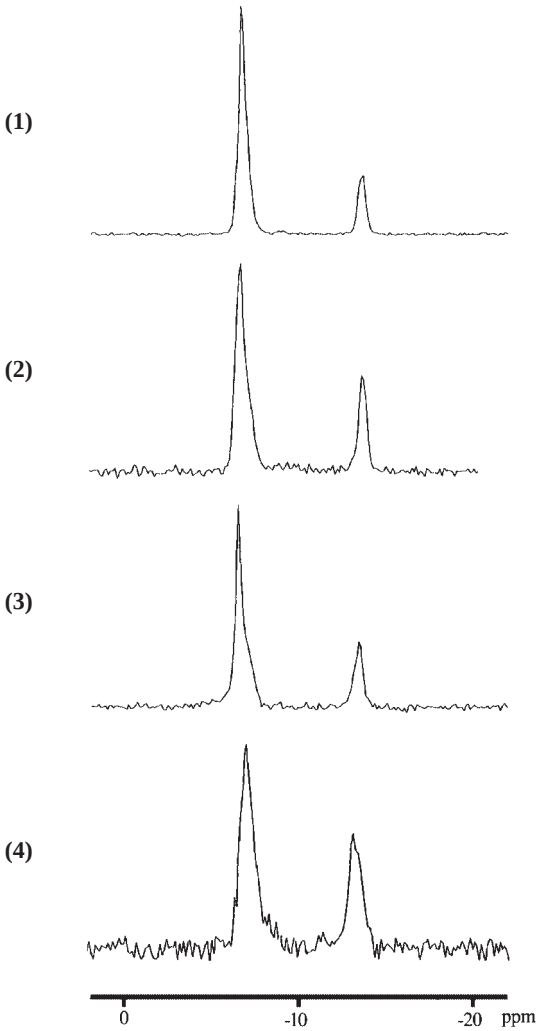

Fig. 5. Solid-state ^{31}P NMR spectra of **1**, **2**, **3**, and **4**.

Solid-State ^{31}P NMR Spectra. The solid-state ^{31}P NMR spectra for **1**–**4** (Fig. 5) had two peaks at δ −6.72 and −13.70, δ −6.72 and −13.57, δ −6.60 and −13.45, and δ −7.21 and −13.21, respectively. The downfield resonance was assigned to the phosphorus closest to the Ti_3 cap, whereas the upfield resonance was assigned to the phosphorus closer to the W_3 cap. The apparent intensity ratio different from the anticipated 1:1 ratio may be attributed to the different relaxation time of two phosphorus resonances in the present POM. The two-line solid-state ^{31}P NMR spectra are consistent with the X-ray crystallography.

Solution ^{31}P NMR Spectra. The ^{31}P NMR spectra in DMSO-d_6 (Fig. 6, Table 2) of **1**–**4** showed two resonances at δ −6.82 and −13.61, δ −6.74 and −13.50, δ −7.06 and −13.33, and δ −7.16 and −13.20, respectively, which agree to the solid-state ^{31}P NMR and are consistent with the X-ray structure analyses. Thus, POMs **1**–**4** are stable in an organic solvent. On the other hand, the ^{31}P NMR spectra in D_2O

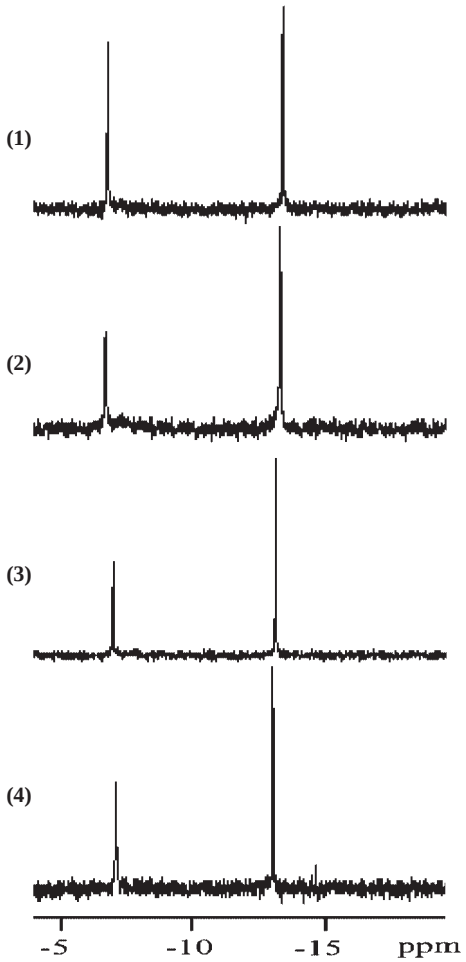

Fig. 6. ^{31}P NMR spectra in DMSO-d_6 of **1**, **2**, **3**, and **4**.

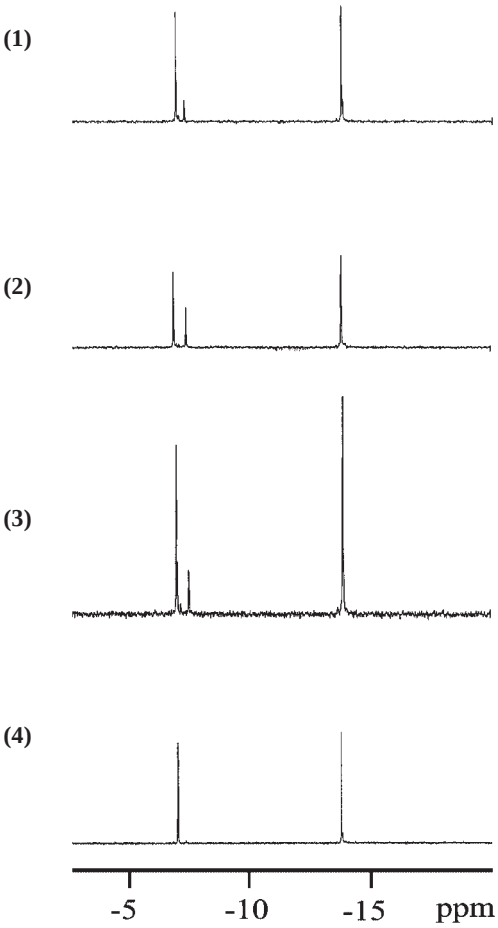

Fig. 7. ^{31}P NMR spectra in D_2O of **1**, **2**, **3**, and **4**.

Table 2. Solid-State and Solution ^{31}P NMR Data of **1a**–**6a**

	Solid-state	DMSO-d_6	D_2O	
			Major peaks	Minor peaks
(1) The tetrameric POM with the bridging Ti octahedral groups				
X = Br (**1a**):	−6.72, −13.70	−6.82, −13.61	−6.93, −13.79	−7.03, −7.27
X = I (**2a**):	−6.72, −13.57	−6.74, −13.50	−6.81, −13.82	−7.33
X = NO_3 (**3a**):	−6.60, −13.45	−7.06, −13.33	−6.96, −13.90	−7.12, −7.46
X = Cl (**4a**):	−7.21, −13.21	−7.16, −13.20	−7.04, −13.77	none
(2) The tetrameric POM without the bridging Ti octahedral groups				
X = Cl (**5a**):			−7.59, −13.97	
X = none, i.e. without X ion (**6a**):			−7.3, −13.8	

(Fig. 7, Table 2) of **1**–**3** showed some minor peaks in addition to the two major resonances: the main peaks at δ −6.93, −13.79 and the minor peaks at δ −7.03, −7.27 for **1**, the main peaks at δ −6.81, −13.82 and the minor peak at δ −7.33 for **2**, and the main peaks at δ −6.96, −13.90 and the minor peaks at δ −7.12, −7.46 for **3**. These spectra in D_2O are different from that of **4** in D_2O, which showed only two peaks at δ −7.04 and −13.77 without any minor peaks.[5a] The ^{31}P NMR minor peaks observed in the spectra of **1**–**3** in water increased to become main signals upon heating the aqueous solution, independent of the encapsulated ions.

We also measured the IR spectra of **1**, **3**, and **4** in aqueous solutions by using the ATR method (Fig. 1b) and those of the samples after heating. Both the IR specra before and after heating were very similar, suggesting that both the major peaks and minor peaks observed by ^{31}P NMR in aqueous solutions at room temperature are probably due to the tetrameric species. Thus, it is suggested that POMs **1**–**3**, as well as **4**, in water

change upon heating to the Cl^- ion-free species, e.g., **6a** without the bridging Ti groups.[3b] On the other hand, it is likely that at room temperature, POMs **1**–**3** in water are less stable than **4**, i.e., the stability in water of POMs strongly depends upon the encapsulated anion. Here, it should be also noted that both in the solid-state and in DMSO-d_6 ^{31}P NMR spectra, the downfield resonances of **4** are at a much higher field than those of **1**–**3**. These facts may be related to the remarkable stability of **4** in the solid-state and in (organic and aqueous) solution.

Conclusion

The "tetrapod"-shaped POMs encapsulating the different anions, $Na_{21-x}H_x[\mathbf{A}]\cdot yH_2O$ ($\mathbf{A} = [\{P_2W_{15}Ti_3O_{59}(OH)_3\}_4\{\mu_3\text{-}Ti(H_2O)_3\}_4X]^{21-}$) X = Br^- (**1**), I^- (**2**), and NO_3^- (**3**) were prepared according to the molecular design, and fully characterized with elemental analysis, thermogravimetric and differential thermal analyses (TG/DTA), solid-state and solution IR, solid-state and solution ^{31}P NMR spectroscopy, and X-ray crystallography.

BVS calculations of the oxygen atoms in **1a**–**3a** showed the following: (1) the bridging Ti octahedral groups are coordinated by water, i.e., they are $Ti(H_2O)_3$ moieties and, not $Ti(OH)_3$ moieties, and (2) all oxygen atoms of T–O–Ti bridges of the Ti_3 cap within the Dawson units, but not those between the Dawson units, are singly protonated.

Encapsulation of the different anions (Cl^-, Br^-, I^-, and NO_3^-) in the central cavity of the giant "tetrapod"-shaped POM shows the cationic character of the central framework constituted by the protonated Ti–O–Ti bonds, i.e., the Ti–OH–Ti bonds. This fact suggests that encapsulation of a cationic species in the central cavity of the POM should be possible by preparing the POM with a central framework constructed with deprotonated Ti–O–Ti bonds, that is, anionic in nature. If this is the case, molecular design of the giant POM molecules would be further extended. Work in this direction and studies on the selectivity of encapsulated anions and other possible anions, which can be encapsulated, are in progress, and the data will be reported in due course.

This work was supported by a Grant-in-Aid for Scientific Research (C) No. 18550062 and also by a High-tech Research Center Project, both from the Ministry of Education, Culture, Sports, Science and Technology, Japan.

Supporting Information

X-ray crystallographic files in CIF format, selected bond distances (Å) and angles (°) around the titanium(IV) centers for the Dawson-POM unit A in **1**–**3** (Tables S1–S3), average bond distances (Å) and angles (°) [range] for the Dawson-POM unit A in **1**–**3** (Tables S4–S6), bond valence sum (BVS) calculations of W, Ti, P, and O atoms (Tables S7–S9), bond distances (Å) and angles (°) of the encapsulated NO_3^- ion (Table S3), and BVS data of the N and O atoms (Table S9). This material is available free of charge on the web at http://www.csj.jp/journals/bcsj/.

References

1 a) M. T. Pope, A. Müller, *Angew. Chem., Int. Ed. Engl.* **1991**, *30*, 34. b) M. T. Pope, *Heteropoly and Isopoly Oxometalates*, Springer-Verlag, New York, **1983**. c) V. W. Day, W. G. Klemperer, *Science* **1985**, *228*, 533. d) C. L. Hill, *Chem. Rev.* **1998**, *98*, 1. e) T. Okuhara, N. Mizuno, M. Misono, *Advances in Catalysis*, **1996**, Vol. 41, p. 113. f) C. L. Hill, C. M. Prosser-McCartha, *Coord. Chem. Rev.* **1995**, *143*, 407. g) A series of 34 papers in a volume devoted to polyoxoanion in catalysis. C. L. Hill, *J. Mol. Catal.* **1996**, *114*, 1. h) R. Neumann, *Progress in Inorganic Chemistry*, **1998**, Vol. 47, p. 317. i) *Polyoxometalate Chemistry from Topology via Self-Assembly to Applications*, ed. by M. T. Pope, A. Müller, Kluwer Academic Publishers, Netherlands, **2001**. j) *Polyoxometalate Chemistry for Nano-Composite Design*, ed. by T. Yamase, M. T. Pope, Kluwer Academic Publishers, Netherlands, **2002**. k) M. T. Pope, *Polyoxo Anions: Synthesis and Structure* in *Comprehensive Coordination Chemistry II*, ed. by A. G. Wedd, Elsevier Science, New York, **2004**, Vol. 4, p. 635. l) C. L. Hill, *Polyoxometalates: Reactivity* in *Comprehensive Coordination Chemistry II*, ed. by A. G. Wedd, Elsevier Science, New York, **2004**, Vol. 4, p. 679. m) A series of 32 recent papers in a volume devoted to Polyoxometalates in Catalysis. C. L. Hill, *J. Mol. Catal.* **2007**, *262*, 1.

2 a) P. J. Domaille, W. H. Knoth, *Inorg. Chem.* **1983**, *22*, 818. b) T. Ozeki, T. Yamase, *Acta Crystallogr., Sect. C* **1991**, *47*, 693. c) W. H. Knoth, P. J. Domaille, D. C. Roe, *Inorg. Chem.* **1983**, *22*, 198. d) T. Yamase, T. Ozeki, S. Motomura, *Bull. Chem. Soc. Jpn.* **1992**, *65*, 1453. e) Y. Lin, T. J. R. Weakley, B. Rapko, R. G. Finke, *Inorg. Chem.* **1993**, *32*, 5095. f) T. Yamase, T. Ozeki, H. Sakamoto, S. Nishiya, A. Yamamoto, *Bull. Chem. Soc. Jpn.* **1993**, *66*, 103. g) K. Nomiya, M. Takahashi, K. Ohsawa, J. A. Widegren, *J. Chem. Soc., Dalton Trans.* **2001**, 2872. h) K. Nomiya, M. Takahashi, J. A. Widegren, T. Aizawa, Y. Sakai, N. C. Kasuga, *J. Chem. Soc., Dalton Trans.* **2002**, 3679. i) O. A. Kholdeeva, G. M. Maksimov, R. I. Maksimovskaya, L. A. Kovaleva, M. A. Fedotov, V. A. Grigoriev, C. L. Hill, *Inorg. Chem.* **2000**, *39*, 3828. j) F. Hussain, B. S. Bassil, L.-H. Bi, M. Reicke, U. Kortz, *Angew. Chem., Int. Ed.* **2004**, *43*, 3485.

3 a) N. J. Crano, R. C. Chambers, V. M. Lynch, M. A. Fox, *J. Mol. Catal.* **1996**, *114*, 65. b) U. Kortz, S. S. Hamzeh, A. Nasser, *Chem. Eur. J.* **2003**, *9*, 2945. c) H. Murakami, K. Hayashi, I. Tsukada, T. Hasegawa, S. Yoshida, R. Miyano, C. N. Kato, K. Nomiya, *Bull. Chem. Soc. Jpn.* **2007**, in prees.

4 a) K. Wassermann, M. H. Dickman, M. T. Pope, *Angew. Chem., Int. Ed. Engl.* **1997**, *36*, 1445. b) U. Kortz, F. Hussain, M. Reicke, *Angew. Chem., Int. Ed.* **2005**, *44*, 2. c) E. Cadot, M.-A. Pilette, J. Marrot, F. Secheresse, *Angew. Chem., Int. Ed.* **2003**, *42*, 2173. d) A. J. Gaunt, I. May, D. Collison, K. T. Holman, M. T. Pope, *J. Mol. Struct.* **2003**, *656*, 101. e) S. S. Mal, U. Kortz, *Angew. Chem., Int. Ed.* **2005**, *44*, 3777. f) G.-S. Kim, H. Zeng, D. VanDerveer, C. L. Hill, *Angew. Chem., Int. Ed.* **1999**, *38*, 3205.

5 a) Y. Sakai, K. Yoza, C. N. Kato, K. Nomiya, *Chem. Eur. J.* **2003**, *9*, 4077. As for the protonation sites within the tetrameric Dawson POMs found with BVS calculations of the oxygen atoms, see also Ref. 6 cited in Ref. 5d. b) Y. Sakai, K. Yoza, C. N. Kato, K. Nomiya, *Dalton Trans.* **2003**, 3581. c) K. Nomiya, Y. Arai, Y. Shimizu, M. Takahashi, T. Takayama, H. Weiner, T. Nagata, J. A. Widegren, R. G. Finke, *Inorg. Chim. Acta* **2000**, *300–302*, 285. d) Y. Sakai, Y. Kitakoga, K. Hayashi, K. Yoza, K. Nomiya, *Eur. J. Inorg. Chem.* **2004**, 4646. e) H. Hori, K. Koike, Y. Sakai, H. Murakami, K. Hayashi, K. Nomiya, *Energy Fuels* **2005**, *19*, 2209.

6 See Supporting Information (Fig. S1) in Ref. 5d.

7 a) K. Hayashi, M. Takahashi, K. Nomiya, *Dalton Trans.*

2005, 3751. b) C. N. Kato, K. Hayashi, S. Negishi, K. Nomiya, *J. Mol. Catal. A* **2007**, *262*, 25. c) K. Hayashi, H. Murakami, K. Nomiya, *Inorg. Chem.* **2006**, *45*, 8078.

8 W. J. Randall, M. W. Droege, N. Mizuno, K. Nomiya, T. J. R. Weakley, R. G. Finke, *Inorganic Syntheses*, **1997**, Vol. 31, p. 167.

9 a) G. M. Sheldrick, *Acta Crystallogr., Sect. A* **1990**, *46*, 467. b) G. M. Sheldrick, *SHELXL-97: Program for Crystal Structure Refinement*, University of Göttingen, Germany, **1997**. c) G. M. Sheldrick, *SADABS*, University of Göttingen, Germany, **1996**.

10 C. Rocchiccioli-Deltcheff, R. Thouvenot, *Spectrosc. Lett.* **1979**, *12*, 127.

11 V. Luzzati, *Acta. Crystallogr.* **1951**, *4*, 239.

12 a) I. D. Brown, D. Altermatt, *Acta Crystallogr., Sect. B* **1985**, *41*, 244. b) I. D. Brown, R. D. Shannon, *Acta Crystallogr., Sect. A* **1973**, *29*, 266. c) I. D. Brown, *Acta Crystallogr., Sect. B* **1992**, *48*, 553. d) I. D. Brown, *J. Appl. Crystallogr.* **1996**, *29*, 479.